

See discussions, stats, and author profiles for this publication at: <https://www.researchgate.net/publication/224853582>

Order Parameters $\langle P-2 \rangle$, $\langle P-4 \rangle$, and $\langle P-6 \rangle$ of Aligned Nematic Liquid-Crystalline Polymer As Determined by Numerical Simulation of Electron Paramagnetic Resonance Spectra

ARTICLE in THE JOURNAL OF PHYSICAL CHEMISTRY B · APRIL 2012

Impact Factor: 3.3 · DOI: 10.1021/jp301170b · Source: PubMed

CITATIONS

6

READS

35

3 AUTHORS:



Tatiana S. Yankova

Lomonosov Moscow State University

16 PUBLICATIONS 94 CITATIONS

SEE PROFILE



Alexey Bobrovsky

Lomonosov Moscow State University

142 PUBLICATIONS 1,724 CITATIONS

SEE PROFILE



Andrey Vorobiev

Lomonosov Moscow State University

42 PUBLICATIONS 311 CITATIONS

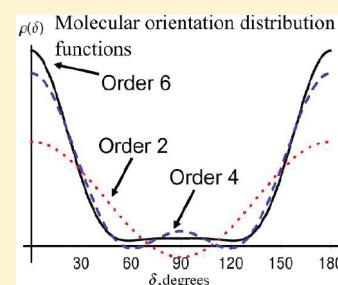
SEE PROFILE

Order Parameters $\langle P_2 \rangle$, $\langle P_4 \rangle$, and $\langle P_6 \rangle$ of Aligned Nematic Liquid-Crystalline Polymer As Determined by Numerical Simulation of Electron Paramagnetic Resonance Spectra

T. S. Yankova,* A. Yu. Bobrovsky, and A. Kh. Vorobiev

Department of Chemistry, Lomonosov Moscow State University, 119991 Moscow, Leninskiye gory, 1/3, Russia

ABSTRACT: High rank order parameters may comprise substantial information about molecular orientational distribution of liquid-crystalline materials. There are few experimental procedures targeted at the determination of high rank order parameters. We suggest a procedure for the determination of order parameters of a spin probe by numerical simulation of electron paramagnetic resonance (EPR) spectra. The procedure is based on revealing the molecular orientation axis of a spin probe. Order parameters $\langle P_2 \rangle$, $\langle P_4 \rangle$, and $\langle P_6 \rangle$ of the spin probe in aligned liquid-crystalline polymer have been measured by the suggested procedure. It was shown that the procedure gives more reliable and complete characteristics of molecular order than does polarized UV–visible spectroscopy.



1. INTRODUCTION

Liquid-crystalline polymers with mesogenic side groups have attracted the attention of researchers for the last three decades.^{1–4} Such kind of materials combines properties of low-molecular liquid crystal and polymer. Thus, they are interesting objects from both scientific and technological viewpoints.

Mesogenic side groups of liquid-crystalline polymer can be aligned by applying external field (magnetic, electrical, or mechanical). Nowadays, there is a wide scope of physical methods that are able to give information about liquid-crystalline order. Among them are polarized UV–visible spectroscopy,^{5–8} polarized fluorescence,^{7–11} polarized Raman spectroscopy,^{12,13} X-rays diffraction,^{14–16} neutron scattering,¹⁷ NMR,^{18,19} EPR,^{20–22} etc. In this work, we are focused on methods that utilize the so-called “guest–host” effect. It is EPR spectroscopy and polarized UV–visible absorption of intentionally introduced admixtures. Liquid-crystalline matrix acts as a host, while molecules of dichroic dye or spin probe are the guests.

Liquid-crystalline orientational order can be completely characterized by an orientation distribution function $\rho(\Omega)$, which gives the probability of finding a molecule at a particular orientation Ω to the liquid-crystal director.^{7,23,24} Here, the set of Euler angles Ω defines the relative orientation of the liquid-crystalline director and the molecular orientation axes. Molecular orientation axes imply principal axes of orientation tensor of rank 2, as it was described in ref 7. If the liquid-crystalline medium is uniaxial, which is typical for aligned nematic phases, and the probe molecules have uniaxial molecular orientation tensor, then the orientation distribution function will depend on the one angle δ between the director and orientation axis (often it is called “long” axis) of the probe molecule. In this case, the distribution function can be expanded in a series of the Legendre polynomial functions $P_l(\cos \delta)$:^{20,23,24}

$$\rho(\delta) = \sum_{l=0}^{\infty} \frac{2l+1}{2} \langle P_l(\cos \delta) \rangle P_l(\cos \delta) \quad (1)$$

where angular brackets denote averaging over all of the molecules. In case of uniaxial molecules with an inversion center the odd terms are equal to zero, and the first few coefficients of expansion are as follows:

$$\begin{aligned} \langle P_0(\cos \delta) \rangle &= 1 \\ \langle P_2(\cos \delta) \rangle &= \frac{1}{2} (3 \langle \cos^2(\delta) \rangle - 1) \\ \langle P_4(\cos \delta) \rangle &= \frac{1}{8} (35 \langle \cos^4(\delta) \rangle - 30 \langle \cos^2(\delta) \rangle + 3) \\ \langle P_6(\cos \delta) \rangle &= \frac{1}{16} (231 \langle \cos^6(\delta) \rangle - 315 \langle \cos^4(\delta) \rangle \\ &\quad + 105 \langle \cos^2(\delta) \rangle - 5) \end{aligned} \quad (2)$$

The function $\rho(\delta)$ is completely specified if all order parameters $\langle P_l \rangle$ are known.⁷

Evidently, the more order parameters are known, the more fine features of the orientation distribution function can be revealed. Lower order parameters can be determined experimentally. Polarized UV–visible spectroscopy that is widely used for characterization of orientation in liquid-crystalline media gives only $\langle P_2 \rangle$ order parameter of dichroic dye dissolved in liquid-crystalline matrix. It is determined by the following formula:^{1,5}

$$\langle P_2 \rangle^{\text{UV}} = \frac{A_{\text{par}} - A_{\text{per}}}{A_{\text{par}} + 2A_{\text{per}}} \times \frac{1}{P_2(\cos \chi)} \quad (3)$$

Received: February 6, 2012

Revised: April 25, 2012

Published: April 26, 2012

Here, A_{par} and A_{per} are the absorbances at parallel and perpendicular polarization directions of a probe beam relative to the sample director, respectively, and angle χ is the angle between the dipole transition moment direction and orientation axis of the dye molecule.

Hence, the drawbacks of polarized UV–visible spectroscopy for characterization of orientation are as follows: (i) for correct determination of order parameter, one needs to know angle χ , or should choose dyes with χ close to zero, and (ii) only $\langle P_2 \rangle$ can be determined.

EPR spectroscopy (spin probe and spin label method) is rather widely used for study of dynamics and orientational order in liquid crystals.^{20–22,25–28} At present, parameters of distribution function can be determined by numerical fitting of experimental EPR spectra. Most often, an orientation distribution function is expressed as a priori mathematical expression based on Boltzmann's distribution law with the orientation-dependent potentials. The software described in refs 22,29 is used for these purposes. It takes into account rotational diffusion of the probe in the field of orienting potential. This approach is mainly targeted on the spin probe (label) molecular dynamics study and is not optimized for the determination of high rank order parameters.

Here, we suggest a procedure for the determination of order parameters $\langle P_2 \rangle$, $\langle P_4 \rangle$, and higher rank order parameters using EPR spectroscopy (spin probe method). The procedure of numerical simulation of EPR spectra gives order parameters of molecular orientation axis of the spin probe. Model-free expansion of orientation distribution function (1) is utilized. The assumptions we imply are uniaxial ODF and uniaxial molecular orientation tensor of spin probes.

The procedure is applied to study the order of liquid-crystalline comb-like polymer with mesogenic side groups (Figure 1a). The structure of the nitroxide spin probe used is



Figure 1. (a) LC-polymer, (b) spin probe, where $R = C_4H_9$, and (c) merocyanine dye ASH253a.

shown in Figure 1b. The molecules are rodlike with rigid central core. Earlier, this compound was found to be an orientation-sensitive spin probe.^{30,31} Merocyanine dye^{32,33} (Figure 1c) was used as the optical probe to compare the order parameters from EPR measurements with optical dichroism.

2. EXPERIMENTAL AND THEORETICAL METHODS

2.1. Materials. Comb-like polymer containing racemic menthyl moieties and nematogenic phenylbenzoate moieties was synthesized according to the method in ref 34. The structure of the polymer is shown in Figure 1a. The polymer

exhibits nematic mesophase. The determined phase transition temperatures are $T_g = 298$ – 303 K, $T_{N-I} = 388$ – 390 K. We have selected such polymer for investigations because menthyl fragment is intrinsically chiral. Yet for the first experiments, copolymer having racemic menthyl groups was synthesized to obtain the simplest nematic phase. Our future work will be concentrated on cholesteric copolymers with nonracemic menthyl-containing fragments.

Stable nitroxide radical 2,5-dimethyl-2-butyloxyphenyl-5-[4-(4-butyloxybenzenecarbonyloxy)phenyl]-pyrrolidine-1-oxide (Figure 1b) was synthesized as described elsewhere³⁵ and kindly granted by Prof. R. Tamura (Kyoto University). We have chosen this spin probe because it bears phenylbenzoate nematogenic moiety as well as the studied polymer. Such similarity may lead to perfect alignment of the probe in the liquid-crystalline medium. Merocyanine dye ASH253a (Figure 1c) was kindly granted to us by Prof. Shirinyan. The synthesis procedure is described in ref 36.

2.2. Sample Preparation. The polymer was added to a chloroform solution of the nitroxide and the dye. The solvent was evaporated, and the obtained material was evacuated at 10^{-3} Torr for several hours on heating to 353 K. Concentrations of the spin probe and the dye in the polymer were 1–2 and 0.2 mol %, respectively. Four milligrams of the dry material was placed between two ITO-glass plates, coated with a film of uniaxially rubbed polyimide. Next, the sample was heated at 363 K to spread the material between the plates. To produce alignment, the sample was annealed for 24 h at 363 K, and then it was cooled to 295 K at the speed 0.2 K/min. It should be noted that the concentration of the spin probe did not decrease significantly after long heating. Thermostatting of the samples was realized using the thermoplate Mettler Fp-86. A glassy transparent monodomain sample with linear dimension 3×15 mm and thickness of about 100 μm was obtained as a result. Phase transitions were watched with a polarizing microscope LOMO R-112. The sample was cooled to 77 K soon after preparation (it will be below referred to as “fresh sample”), and angular dependence of EPR spectra at 77 K was registered. Next, the sample was equilibrated for several weeks at room temperature (referred to as “aged sample”). The rest of the measurements were carried out on this sample.

2.3. Linear Dichroism Measurements. UV–visible spectra in polarized light were recorded using spectrophotometers SPECORD M40 and Shimadzu UV-2401PC with a polarizing Glan prism. Water heating glass cell was used for thermostatting of the samples with accuracy ± 1 K.

Optical dichroism values at different temperatures were calculated according to formula 3 using absorption values at wavelength of maximal adsorption (640 nm). Angle χ between the dipole transition moment and orientation axis of the dye molecule was supposed to be zero. For more precise determination of anisotropy axis and optical dichroism values, angular dependencies of absorbance in polarized light were registered (from 0° to 360° with step 10°) at 640 nm.

2.4. EPR Spectra Angular Dependence Registration. EPR spectra were recorded with X-band spectrometer Varian E3. EPR spectra at 77 K were registered using a quartz Dewar filled with liquid nitrogen. Spectra at temperatures above 295 K were recorded using a quartz Dewar tube with air flow. The air flow temperature was maintained with a PID-controller with an accuracy ± 0.5 K. EPR spectra were recorded at different angles between magnetic field vector and the sample anisotropy axis with a 10° step. The sample was turned around the axis

perpendicular both to the magnetic field and to the sample anisotropy axis. Turn angles were set with accuracy $\pm 0.2^\circ$ using a goniometer. The set of spectra obtained in the course of such procedure is referred to below as angular dependence of EPR spectrum. All experimental spectra were normalized so that the double integral of each spectrum was equal to unity.

2.5. EPR Spectra Numerical Simulation. **2.5.1. Reference Frames Used in the Analysis of EPR Spectra.** Reference frames that will be used are shown in Figure 2. We choose the Z axis of

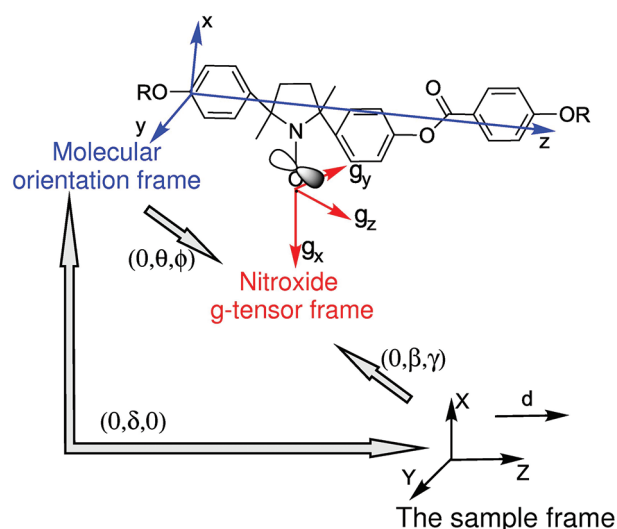


Figure 2. Reference frames and Euler angles used in analysis of EPR spectra.

the sample frame (XYZ) to coincide with the liquid-crystalline director. As far as molecular alignment in the sample and molecular orientation tensor of the spin probes are uniaxial, molecular orientation tensor is related to the sample director by one angle δ . Euler angles $(0, \beta, \gamma)$ relate the sample director frame and the principal axes of g -tensor of the nitroxide spin probe. The relative orientation of molecular orientation tensor (principal orientation axis) and g -tensor principal axes is given by angles $(0, \theta, \phi)$.

2.5.2. Numerical Simulation of EPR Spectra of Disordered Sample. The numerical simulation of EPR spectra included minimization of deviations of calculated spectra from experimental ones (discrepancy). The discrepancy is taken as follows:

$$D = \frac{1}{2} \sum_i \frac{r_i^2}{n} \quad (4)$$

where r_i is the difference of intensities between calculated and experimental spectra, and n is the number of points in the spectrum.

The discrepancy is minimized using an adaptive nonlinear least-squares algorithm described in ref 37. The calculation of EPR spectra was performed in the high-field approximation up to second order of the perturbation theory. Individual line shape was described by convolution of Gaussian and Lorentzian functions. Gaussian and Lorentzian linewidths were second-rank tensors to take into account the anisotropy of the linewidths. The linewidths axes were assumed to coincide with g -tensor principal axes.

The magnetic parameters (components of g -tensor and tensor of hyperfine interaction) of the spin probe were

determined by simulation of EPR spectra of isotropic sample at 77 K at rigid limit conditions. A_x and A_y components values were then refined by simulation at 295 K because at this temperature x - and y -components of the EPR spectrum have better resolution. The following values have been obtained: $g_x = 2.0092 \pm 0.0002$, $g_y = 2.0059 \pm 0.0002$, $g_z = 2.0021 \pm 0.0002$, $A_x = 4.9 \pm 0.3$ G, $A_y = 4.2 \pm 0.3$ G, $A_z = 32.5 \pm 0.2$ G.

Fast stochastic orientational movements of spin probes with the restricted amplitude (quasi-librations) resulting in partial averaging of magnetic parameters of spin probes were taken into account in the course of simulation of spectra recorded at 295, 318, and 326 K. In the present work, we used expressions for averaging of magnetic resonance parameters when librations occurred around an arbitrary molecular axis of a spin probe (or spin label).³⁸ Librations axes of the spin probe in this case are assumed to coincide with principal axes of molecular orientation tensor.

The values of libration amplitudes at different temperatures are shown in Table 1. L_{par} is half amplitude of librations around

Table 1. Libration Amplitudes of the Spin Probe Molecules and Disorder Factors

$T, \text{ K}$	$L_{\text{par}}, \text{ deg}$	$L_{\text{perp}}, \text{ deg}$	$F_{\text{libr}}^{(2)}$	$F_{\text{libr}}^{(4)}$	$F_{\text{libr}}^{(6)}$
295	29.0 ± 0.5	0.0 ± 0.7	1	1	1
318	35.2 ± 1.0	7.5 ± 1.0	0.97	0.92	0.83
326	35.3 ± 1.0	11.5 ± 0.8	0.94	0.81	0.62

the molecular orientation axis, and L_{perp} is half amplitude of librations around axis perpendicular to the molecular orientation axis. From Table 1, one can see that the higher is the temperature, the higher is the libration amplitude. Librations with bigger amplitude occur around the molecular orientation axis of the spin probe. Librations intensity around the axis that is perpendicular to orientational axis (with half amplitude L_{perp}) affects the orientational order of the spin probe molecules. It can be taken into account by disordering factors of second-order $F_{\text{libr}}^{(2)} = P_2(\cos(L_{\text{perp}}))$, fourth-order $F_{\text{libr}}^{(4)} = P_4(\cos(L_{\text{perp}}))$, and sixth-order $F_{\text{libr}}^{(6)} = P_6(\cos(L_{\text{perp}}))$. Values of $F_{\text{libr}}^{(i)}$ at different temperatures are shown in Table 1.

2.5.3. Numerical Simulation of EPR Spectra of the Aligned Sample. The procedure for determination of an orientation distribution function by numerical simulation of angular dependencies of EPR spectra is described in detail in ref 39. The orientation distributions of magnetic axes of spin probes were determined in this work. It is expressed as a series expansion of orthonormalized spherical functions:

$$\rho(\beta, \gamma) = \frac{1}{2\pi} \sum_{l=0}^{\infty} \left(\frac{1}{2} a_{l0} P_l(\cos \beta) + \sum_{k=1}^l P_{lk}(\cos \beta) [a_{lk} \cos k\gamma + b_{lk} \sin k\gamma] \right) \quad (5)$$

where $P_l(\cos \beta)$ is the Legendre polynomial, and $P_{lk}(\cos \beta)$ is the associated Legendre polynomial. Angles (β, γ) relate principal g -tensor axes and the reference frame of the uniaxial sample.

In the present work, we deal with the uniaxial sample, and we assume that the spin probe molecules align uniaxially (i.e., molecular orientation tensor is uniaxial). In this case, the orientation distribution function is uniaxial and can be represented as expansion (1).

It can be shown that expansion coefficients (a_{lk} , b_{lk}) of distribution function (5) are related to order parameters $\langle P_l \rangle^{\text{EPR}}$ of expansion (1) by the following expressions:

$$a_{lk} = \langle P_l(\cos \delta) \rangle_{\text{EPR}} \frac{(2l+1)(-1)^k(l-k)!}{(l+k)!} \cos k\varphi \times P_k(\cos \theta)$$

$$b_{lk} = -\langle P_l(\cos \delta) \rangle_{\text{EPR}} \frac{(2l+1)(-1)^k(l-k)!}{(l+k)!} \sin k\varphi \times P_k(\cos \theta) \quad (6)$$

where Euler angles (θ , φ) relate the orientational axis to g-tensor principal axes of the spin probe molecule.

We modified the procedure of numerical simulation of EPR spectra, described in ref 39. The new procedure is capable of finding angles (θ , φ) and the order parameters $\langle P_l \rangle^{\text{EPR}}$ of molecular orientation axis via least-squares fitting of experimental spectra. Orientation distribution function in the form of truncated series (1) was used in the simulation procedure. Ten EPR spectra of angular dependence were simulated jointly. Values of θ and φ angles were found by simulation of angular dependence of EPR spectra at 77 K (in rigid limit). Next, the simulations of angular dependencies recorded at 295, 318, and 326 K were performed at fixed values of angles (θ , φ) and at fixed magnetic parameters of spin probe (rigid limit values).

Negative values of the orientation distribution function are physically meaningless. To avoid negative values, we imposed the constraint on negative values of the function $\rho(\delta)$ expanded in the series (1) in the course of numerical simulation of EPR spectra. For this purpose, we used the modified minimization function $D' = 1/2 \sum_n (r^2(1 + V_{\text{neg}}K)^2)/n$, where V_{neg} is the negative portion of distribution function, which is calculated as follows:

$$V_{\text{neg}} = \frac{\int_{\delta} |\rho(\delta)| d\delta - \int_{\delta} \rho(\delta) d\delta}{2 \int_{\delta} |\rho(\delta)| d\delta} \quad (7)$$

and K is the penalty factor allowing one to adjust the requirement of distribution function positivity.

If the resulting ODF has nonzero negative portion, the fitting procedure was repeated with increased value of penalty factor K . Eventually this procedure yields a positive orientation distribution function, which corresponds to minimal discrepancy. Stability of the solution was proved by deviation of parameters from optimal values followed by simulation without the constraint on negative values of the ODF.

To choose necessary truncation of the series (1), the following procedure was used:

- Angular dependence of EPR spectrum was recorded twice.
- Differences between amplitudes of corresponding points of two spectra recorded at the same angle ($r'_i - r''_i$) were averaged over all spectra as followed: $S = 1/2 \sum_i ((r'_i - r''_i)^2)/N$, where N is the total number of points in all spectra of angular dependence. Value of S in our experiment was found to be $S = 3.5 \times 10^{-10}$. This value reflects a level of noise, drift of the spectrometer settings, and errors of setting of the angle between magnetic field and the sample anisotropy axis.
- Numerical simulation of experimental EPR spectra was carried out with truncation of the series (1) up to term l

(expansion rank is l), and then simulation was repeated with expansion rank $l+2$. If the difference between optimal minimization functions $D_{l+2} - D_l$ is substantially less than the value of S , the expansion of rank l was considered as enough to fit the EPR spectra. Otherwise, term $l+2$ was added in the series (1).

To estimate the errors of parameters determination, we used standard deviation of noise σ , which is determined from experimental points along the sufficient length of baseline, according to the work in ref 29. Standard deviations of noise for the EPR spectra registered at different temperatures are shown in Table 2.

Table 2. Standard Deviations of the Noise σ

T, K	77	295	318	326
$\sigma \times 10^{11}$	2.6	14.4	24.0	22.0

Statistical error of the parameter is defined as deviation of the parameter value from optimal, which produces an increase of function D by a value of $\sigma^2/2$.

Sometimes the deviation of the parameter from optimal value produced meaningless negative fraction of ODF. If the parameter range of positive ODF was narrower than the statistical error interval, it was used as the error of the determined value of parameter.

3. RESULTS AND DISCUSSION

3.1. Optical Dichroism. Polarized absorbance spectra of the sample recorded in two orientations of the sample anisotropy axis relative to polarization of probe beam are shown in Figure 3a. Maximum absorption of the dye is observed at 640 nm. Optical order parameter was found to be $\langle P_2 \rangle^{\text{UV}} = 0.36 \pm 0.01$ within the temperature interval from 295 to 326 K (see Figure 3b). It demonstrates very weak temperature dependence in the studied temperature range. Angular dependence of polarized absorbance was registered at 640 nm for a more precise determination of the optical dichroism value. The polarized transmittance ($T = 10^{-A}$) is plotted in Figure 4. One can see that the maximum of polarized transmittance slightly deviates from 90° ; it is accounted for by the sample set error. It is known that light intensity depends on the squared cosine of the light polarization angle (Malus's law). The experimental dependence of transmittance was fitted by the function: $T(\varphi) = T_{\text{min}} + T_{\text{max}} \cos^2(\varphi + \delta_0)$, where φ is the light polarization angle, and δ_0 is the sample set error angle. The T_{max} , T_{min} , and δ_0 were fitting parameters. The dichroism value determined by treatment of angular dependence was found to be equal to the value calculated above by use of two spectra within experimental errors.

3.2. High Rank Order Parameters of Orientation Axis. EPR spectra angular dependencies are shown in Figure 5. One can see that EPR spectra recorded at 77 and 326 K are similar, but it was impossible to produce good fitting by use of the same set of parameters at different temperatures. Temperature dependence of EPR spectra was successfully described using librations model, as it is described in section 2.5.2. At first, Euler angles (θ , φ), which specify the direction of the principal orientation axis z with regard to g-tensor principal axes, were determined through the numerical simulation of EPR spectra angular dependence at 77 K. They were found to be $\theta = (32 \pm 2)^\circ$ and $\varphi = (90 \pm 22)^\circ$. Angle θ is the angle between the principal orientation axis and the g_z axis of the g-tensor frame,

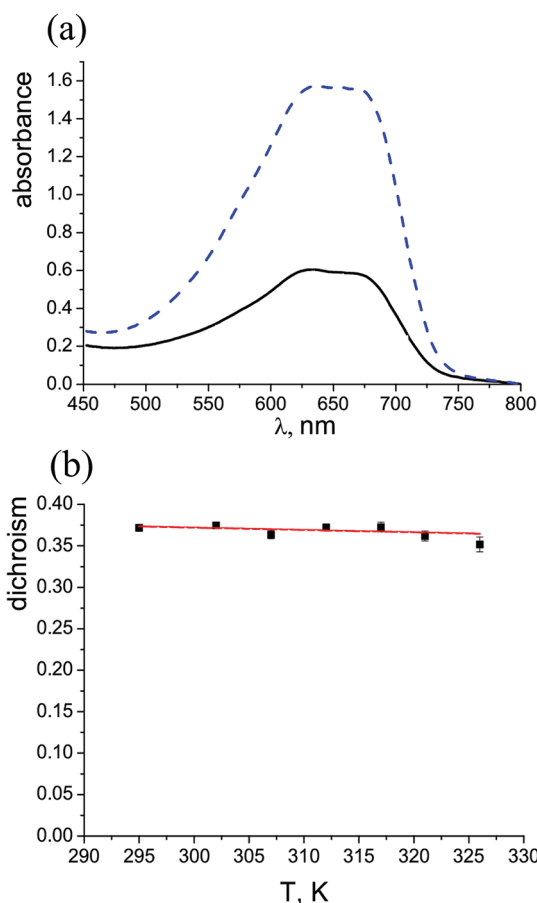


Figure 3. (a) Polarized absorbance spectra of aligned LC polymer doped with the spin probe and merocyanine dye at 295 K, along with parallel (—) and perpendicular (---) relative orientations of the sample director and probe light beam. (b) Temperature dependence of linear dichroism for the sample (■) and its linear fit (—).

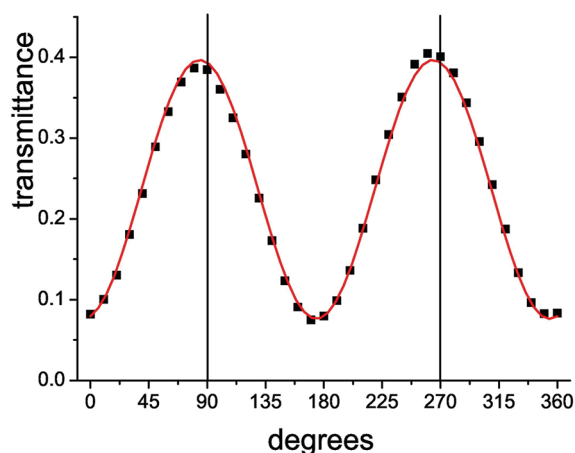


Figure 4. Angular dependence of polarized transmittance at 640 nm at 295 K (■) and its fitting (—).

and angle φ is the angle between projection of the principal orientation axis to $g_x g_y$ plane and the g_x axis. The values of the angles are in agreement with the geometry of the spin probe molecule geometry, which is shown schematically in Figure 2.

Following numerical simulations of angular dependencies of EPR spectra at temperatures 295, 318, and 326 K were carried

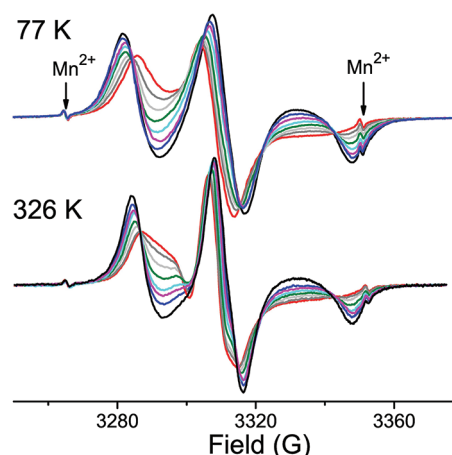


Figure 5. EPR spectra angular dependencies of the nitroxide in aligned LC polymer at 77 and 326 K.

out at fixed values of angles $\theta = 32^\circ$ and $\varphi = 90^\circ$ and fixed values of librations amplitudes, shown in Table 1.

To find out the necessary expansion rank of the series (1), we performed simulation of EPR spectra using expansion rank $l = 2, 4, 6, 8$ and compared the values of minimization function D for these simulations. The resulting D values are shown in Table 3. One can see from the table that the higher is the

Table 3. Minimization Function D Values at Optimal Fitting Parameters, Determined at Different Expansion (1) Rank for Experimental Spectra Recorded at 77 K^a

expansion rank l in the series (1)	$D \times 10^9$	
	"fresh" sample	"aged" sample
2	5.980	3.35
4	2.200	1.75
6	1.902	1.72
8	1.896	

^aLevel of noise $S = 3.5 \times 10^{-10}$.

expansion rank, the lower is the discrepancy achieved. Use of expansion rank 4 leads to a substantial decrease (about 2 times) of the minimization function D . Use of expansion rank 6 led to a smaller decrease of D value as compared to expansion rank 4. In case of "fresh" sample, the decrease of function D is comparable to the value of level noise $S = 3.5 \times 10^{-10}$. Thus, we conclude that order parameters of rank 4 are determined easily from the angular dependence of EPR spectra. Information about order parameter of rank 6 can be recovered from EPR spectra of the "fresh" sample at 77 K, but the accuracy of this value is less. Thus, we performed the numerical simulations for EPR spectra at different temperatures with expansion rank 6. The quality of the EPR spectra (recorded at 295 K) fitting is illustrated in Figure 6.

Optimal values of order parameters determined for the EPR spectra at different temperatures are collected in Table 4. Values of discrepancy D achieved at fitting with expansion rank 4 and rank 6 are given. One can see that the order parameters for the "fresh" sample are bigger than those the "aged" one. Evidently, the process of relaxation of orientation takes place; therefore, the "aged" sample is less ordered than the "fresh sample". As a result, the values of order parameters of rank 6 could not be reliably extracted from EPR spectra of the "aged" sample.

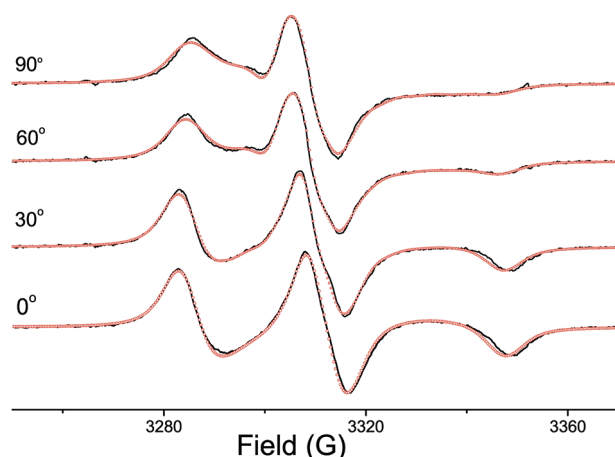


Figure 6. EPR spectra of the spin probe in aligned LC polymer recorded at different angles between anisotropy axis and magnetic field (295 K): experimental spectra (—), numerical simulation (○).

Order parameters $\langle P_l \rangle$ in Table 4 are corrected by libration disordering factors $F_{\text{libr}}^{(l)}$, presented in Table 1. The influence of the librations on the orientational order parameters in our experiments was found to be within experimental errors. Obtained values of order parameters define the orientation distribution function of the spin probe molecules. The function in accordance with (1) describes the distribution of probe orientational axis in the three-dimensional sample frame (Figure 7a). Given order parameters $\langle P_l \rangle$ and angles (θ, φ) , coefficients (a_{lk}, b_{lk}) of distribution (5) can be calculated using formula 6. Function (5) is a distribution of magnetic axes of a spin probe molecule in a uniaxial sample. This function can be visualized as a two-dimensional surface in three-dimensional space only as a distribution of the sample director in the spin probe g -tensor frame (Figure 7b). It is clear that the tilt angle of the symmetry axis of the function in Figure 7b corresponds to angles (θ, φ) and it shows direction of the molecular orientation axis with respect to g -tensor principal axes. The uncertainty of angles (θ, φ) should be mentioned. Because of orthorhombic symmetry of the magnetic system of a spin probe, orientation distribution functions with any set of angles (θ, φ) , $(\theta, \pi - \varphi)$, $(\theta, \pi + \varphi)$, $(\pi - \theta, \varphi)$, etc. are undistinguishable by EPR spectroscopy. We imply this problem and choose one of these sets arbitrarily.

The characteristics of orientational distribution obtained by simulation of EPR spectra can be compared to the data of optical measurements. Typical values of $\langle P_2 \rangle$ for aligned comb-like liquid-crystalline polymers, determined using various experimental techniques,^{2,10,11} lie within interval from 0.45 to 0.65. It is seen from Table 4 that the $\langle P_2 \rangle^{\text{EPR}}$ value determined by EPR spectroscopy is in agreement with the literature data. The value of optical dichroism measured in the present work is

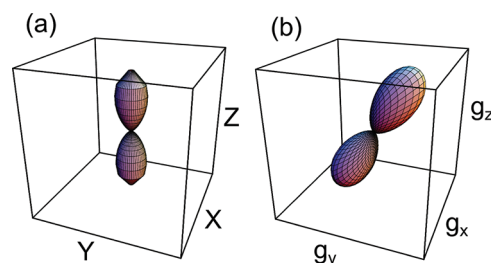


Figure 7. ODFs of the spin probe at 295 K: (a) ODF is represented as the distribution of the orientational axis in the sample frame; (b) ODF is represented as the distribution of the sample anisotropy axis in g -tensor frame.

about 30% less and equal to 0.36 ± 0.01 . We suppose there would be two reasons for this noncoincidence:

- the spin probe molecules are aligned better than the dye molecules;
- the dipole transition moment direction and orientational axis of the dye molecule do not coincide; that is, angle χ (see eq 3) is not zero.

There are few works devoted to experimental determination of high rank order parameters. Values of $\langle P_4 \rangle$ for nematic mesophase determined by polarized Raman spectroscopy, neutron scattering, and X-ray diffraction vary within the interval 0.1–0.3.^{12,13,17} In case of measurements of polarized fluorescence, the negative values of $\langle P_4 \rangle$ are often obtained.^{8,10,11} This feature arises as a result of tilt between absorption and fluorescence dipole transition moments.¹⁰ Thus, the $\langle P_4 \rangle$ values measured by polarized luminescence could hardly be compared to the data of other techniques. To our knowledge, the value of $\langle P_6 \rangle$ was measured for nematic phase only in the work of ref 17. Using the neutron scattering, it was found to be 0.05. Values of $\langle P_4 \rangle^{\text{EPR}}$ and $\langle P_6 \rangle^{\text{EPR}}$ found in the present work are in agreement with the literature data.

The importance of high rank order parameters in the description of the ODF shape is illustrated by two-dimensional plots (Figure 8). The orientation distribution function for the “fresh” sample (Table 4, column 2) is plotted using the expansion rank = 6 (—), 4 (---), and 2 (···). One can see that the distribution plotted with expansion rank 2 only is incorrect as it contains the meaningless negative fractions. Distribution function with the expansion rank 4 and 6 seems to be significantly more reliable. It exhibits a nonzero constant value between $\sim 50^\circ$ and $\sim 130^\circ$, which corresponds to isotropic orientation of some fraction of the molecules in the sample.

4. CONCLUSIONS

Summarizing the obtained results, one can conclude that the procedure for numerical simulation of EPR spectra allows one to determine orientation distribution function and, conse-

Table 4. Order Parameters of the Spin Probe at Different Temperatures

	77 K, “fresh” sample	77 K, “aged” sample	295 K, “aged” sample	318 K, “aged” sample	326 K, “aged” sample
$\langle P_2 \rangle$	0.56 ± 0.01	0.50 ± 0.01	0.56 ± 0.02	0.55 ± 0.03	0.50 ± 0.02
$\langle P_4 \rangle$	0.28 ± 0.01	0.17 ± 0.03	0.16 ± 0.04^a	0.17 ± 0.07	0.14 ± 0.04
$\langle P_6 \rangle$	0.063 ± 0.006	0.013 ± 0.014	0.016 ± 0.032	0.035 ± 0.030^a	0.022 ± 0.019
$D \times 10^9$ for rank 4	2.20	1.73	1.92	2.99	3.25
$D \times 10^9$ for rank 6	1.90	1.72	1.90	2.74	2.93

^aThe parameter range satisfying condition of ODF positivity is presented as an error.

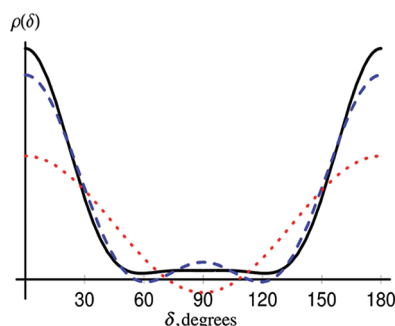


Figure 8. Orientation distribution functions (1), 77 K, for the “fresh” sample, plotted using the expansion rank = 2 (\cdots), 4 ($---$), and 6 ($-$).

quently, high rank order parameters $\langle P_l \rangle$ of the orientational axis of the spin probe molecule. $\langle P_2 \rangle$, $\langle P_4 \rangle$, and $\langle P_6 \rangle$ order parameters for oriented liquid-crystalline comb-like polymer were determined. It turned out that $\langle P_2 \rangle^{\text{EPR}}$ order parameter of the spin probe molecules is higher than the order parameter of the dye molecules $\langle P_2 \rangle^{\text{UV}}$ for the considered polymer. It may be accounted for by the noncoincidence of the dipole transition moment direction and the molecular orientation axis of the dye molecule. $\langle P_4 \rangle^{\text{EPR}}$ and $\langle P_6 \rangle^{\text{EPR}}$ values are in agreement with literature data, known for nematic mesophase. It is shown that the spin probe molecules are rod-like and similar to host matrix molecules; the order parameters of the molecular orientation axis of spin probe reflect the order of host molecules better than the value determined by polarized optical spectroscopy. The high rank order parameters, determined by this procedure, reveal fine details of orientational order.

AUTHOR INFORMATION

Corresponding Author

*Tel.: +7(495)939-49-00. Fax: +7(495)939-00-67. E-mail: ya.tatiana@gmail.com.

Notes

The authors declare no competing financial interest.

ACKNOWLEDGMENTS

This work was supported by the Russian Foundation for Basic Research, grant no. 11-03-01046-a. We thank Prof. R. Tamura for provision of paramagnetic probe and Prof. Shirinyan for provision of the merocyanine dye.

REFERENCES

- (1) Finkelmann, H.; Rehage, G. *Adv. Polym. Sci.* **1984**, *60/61*, 99–172.
- (2) Shibaev, V.; Plate, N. *Adv. Polym. Sci.* **1984**, *60/61*, 173–251.
- (3) Shibaev, V. *Mol. Cryst. Liq. Cryst.* **1994**, *243*, 201–230.
- (4) Donald, A. M.; Windle, A. H.; Hanna, S. *Liquid Crystalline Polymers*; Cambridge University Press: Cambridge, UK, 2006.
- (5) Daniels, J. M.; Cladis, P. E.; Finn, P. L.; Powers, L. S.; Smith, J. C.; Filas, R. W.; Goodby, J. W.; Leslie, T. M. *J. Appl. Phys.* **1982**, *53*, 6127–6136.
- (6) Chigrinov, V. G.; Kozenkov, V. M.; Kwok, H.-S. *Photoalignment of Liquid Crystalline Materials*; West Sussex PO19 8SQ: England, 2008.
- (7) Michl, J.; Thulstrup, E. W. *Spectroscopy with Polarized Light: Solute Alignment by Photoselection. Liquid Crystals, Polymers and Membranes*; VCH Publishers: New York, 1986.
- (8) Bauman, D.; Chrzumnicka, E.; Wolarz, E. *Mol. Cryst. Liq. Cryst.* **2000**, *352*, 67–76.
- (9) Chapoy, L. L.; DuPre, D. B. *J. Chem. Phys.* **1979**, *70*, 2550–2553.
- (10) Wolarz, E.; Bauman, D. *J. Polym. Sci., Part B: Polym. Phys.* **1993**, *31*, 383–387.
- (11) Wolarz, E.; Chrzumnicka, E.; Fischer, T.; Stumpe, J. *Dyes Pigm.* **2007**, *75*, 753–760.
- (12) Southern, C. D.; Brimicombe, P. D.; Siemianowski, S. D.; Jaradat, S.; Roberts, N.; Goertz, V.; Goodby, J. W.; Gleeson, H. F. *EPL* **2008**, *82*, S6001.
- (13) Sanchez-Castillo, A.; Osipov, M.; Giesselmann, F. *Phys. Rev. E* **2010**, *81*, 021707.
- (14) Deutsch, M. *Phys. Rev. A* **1991**, *44*, 8264–8270.
- (15) Davidson, P. *Prog. Polym. Sci.* **1996**, *21*, 893–950.
- (16) Giesselmann, F.; Germer, R.; Saipa, A. *J. Chem. Phys.* **2005**, *123*, 034906.
- (17) Hamley, I. W.; Luckhurst, G. R.; Richardson, R. M.; Santos, F. J. *Chem. Phys.* **2002**, *116*, 3887–3899.
- (18) Domenici, V. *Pure Appl. Chem.* **2007**, *79*, 21–37.
- (19) Titman, J.; Féaux de Lacroix, S.; Spiess, H. W. *J. Chem. Phys.* **1993**, *98*, 3816–3826.
- (20) Luckhurst, G.; Yeates, R. N. *J. Chem. Soc., Faraday Trans. 2* **1976**, *72*, 996–1009.
- (21) Freed, J. H. In *Spin Labeling: Theory and Applications*; Berliner, L. J., Ed.; Plenum Press: New York, 1976.
- (22) Schneider, D. J.; Freed, J. H. In *Biological Magnetic Resonance*; Berliner, L. J., Reuben, J., Eds.; Plenum: New York, 1989.
- (23) Zannoni, C. In *The Molecular Physics of Liquid Crystals*; Luckhurst, G. R., Gray, G. W., Eds.; Academic Press: New York, 1979.
- (24) Blinov, L. *Structure and Properties of Liquid Crystals*; Springer Science Business Media B.V.: New York, 2011.
- (25) Meirovitch, E.; Igner, D.; Igner, E.; Mora, G.; Freed, J. H. *J. Chem. Phys.* **1982**, *77*, 3915–3938.
- (26) Wassmer, K. H.; Ohmes, E.; Portugall, M.; Ringsdorf, H.; Kothe, G. *J. Am. Chem. Soc.* **1985**, *107*, 1511–1519.
- (27) Xu, D.; Budil, D. E.; Ober, C. K.; Freed, J. H. *J. Phys. Chem.* **1996**, *100*, 15867–15872.
- (28) Imrie, C. T.; Ionescu, D.; Luckhurst, G. R. *Macromolecules* **1997**, *30*, 4597–4600.
- (29) Budil, D. E.; Lee, S.; Saxena, S.; Freed, J. H. *J. Magn. Reson., Ser. A* **1996**, *120*, 155–189.
- (30) Chumakova, N. A.; Vorobiev, A. Kh.; Ikuma, N.; Uchida, Y.; Tamura, R. *Mendeleev Commun.* **2008**, *18*, 21–23.
- (31) Chumakova, N. A.; Pomogailo, D. A.; Yankova, T. S.; Vorobiev, A. Kh. *Mol. Cryst. Liq. Cryst.* **2011**, *540*, 196–204.
- (32) Bobrovsky, A.; Shibaev, V.; Elyashevitch, G.; Rosova, E.; Shimkin, A.; Shirinyan, V.; Bubnov, A.; Kaspar, M.; Hamplova, V.; Glogarova, M. *Liq. Cryst.* **2008**, *35*, 533–539.
- (33) Bobrovsky, A.; Ryabchun, A.; Shibaev, V. *J. Photochem. Photobiol., A* **2011**, *218*, 137–142.
- (34) Bobrovsky, A. Yu.; Boiko, N. I.; Shibaev, V. P. *Polym. Sci., Ser. A* **1998**, *40*, 232–239.
- (35) Ikuma, N.; Tamura, R.; Shimono, S.; Uchida, Y.; Masaki, K.; Yamauchi, J.; Aoki, Y.; Nohira, H. *Adv. Mater.* **2006**, *18*, 477–480.
- (36) Shimkin, A. A.; Shirinian, V. Z.; Nikalin, D. M.; Krayushkin, M. M.; Pivina, T. S.; Troitsky, N. A.; Vorontsova, L. G.; Starikova, Z. A. *Eur. J. Org. Chem.* **2006**, *9*, 2087–2092.
- (37) Dennis, J. E.; Gay, D. M.; Welsch, R. E. *Trans. Math. Software* **1981**, *7*, 348–368.
- (38) Timofeev, V.; Samarianov, B. *J. Chem. Soc., Perkin Trans. 2* **1995**, 2175–2181.
- (39) Vorobiev, A. Kh.; Chumakova, N. A. *J. Magn. Reson.* **2005**, *175*, 146–157.